Biomacromolecules

Article

Cite This: Biomacromolecules 2019, 20, 1505−1513

pubs.acs.org/Biomac

Molecular Characterization of Mucus Binding

Jacob Witten,[†,‡] Tahoura Samad,[†] and Katharina Ribbeck*[,†]

[†]Department of Biological Engineering and [‡]Computational and Systems Biology Initiative, Massachusetts Institute of Technology, Cambridge, Massachusetts 02139, United States

Supporting Information

ABSTRACT: Binding of small molecules to mucus membranes in the body has an important role in human health, as it can affect the diffusivity and activity of any molecule that acts in a mucosal environment. The binding of drugs and of toxins and signaling molecules from mucosal pathogens is of particular clinical interest. Despite the importance of mucus−small molecule binding, there is a lack of data revealing the precise chemical features of small molecules that lead to mucus binding. We developed a novel equilibrium dialysis assay to measure the binding of libraries of small molecules to mucin and other mucus components, substantially increasing the throughput of small molecule binding measurements. We validated the biological relevance of our approach by quantifying binding of the antibiotic colistin to mucin, and showing that this binding was associated with inhibition of colistin's bioactivity. We next used a small molecule microarray to identify 2,4-diaminopyrimidine as a mucin binding motif and confirmed the importance of this motif for mucin binding using equilibrium dialysis. Furthermore, we showed that, for molecules with this motif, binding to mucins and the mucus-associated biopolymers DNA and alginate is modulated by differences in hydrophobicity and charge. Finally, we showed that molecules lacking the motif exhibited different binding trends from those containing the motif. These results open up the prospect of routine testing of small molecule binding to mucus and optimization of drugs for clinically relevant mucus binding properties.

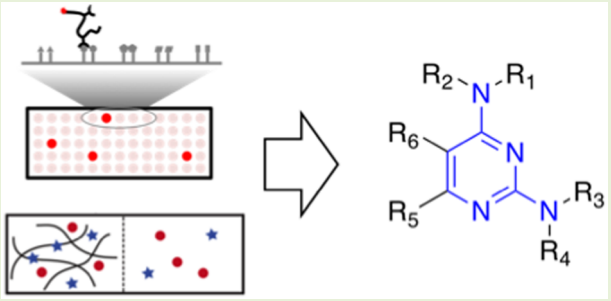

INTRODUCTION

Mucus is a viscoelastic hydrogel layer that coats every nonkeratinized epithelial surface of the body, including the lungs and intestines.[1] Its activity has important ramifications for biology and medicine:[2−5] the selective binding of small molecules to mucus may affect the activity and diffusivity of any molecule acting in a mucosal environment.[3] Medically relevant molecules affected by mucus include bacterially produced toxins and signaling molecules and inhaled therapeutics for diseases including cystic fibrosis (CF), chronic obstructive pulmonary disease (COPD), and asthma.[2,3]

The main gel-forming components of mucus are large secreted glycoproteins called mucins, which contain alternating regions of globular hydrophobic domains and disordered polyanionic oligosaccharide brushes with sialic acid and sulfated groups.[1,6] Since mucins are a major component of mucus, the ability of a molecule to bind to mucin is a key determinant of mucus binding. Mucin overproduction is a hallmark of respiratory diseases including CF, COPD, and asthma,[7] suggesting that mucin binding is correspondingly more important in these pathologies. Synthetically cross-linked, purified mucin gels are a second environment in which mucin binding plays a role; they are a promising biomaterial for sustained drug delivery, and mucin binding helps determine the kinetics of drug release.[8] Mucins can also nonenzymatically catalyze some organic reactions by binding to relevant molecules.[9]

Besides mucins, lung mucus contains lipids, proteins, extracellular DNA (eDNA), and bacterial polysaccharides (e.g., the polyanion alginate, often present in infections by the *Pseudomonas aeruginosa*, an opportunistic pathogen[10]). Both eDNA and bacterial polysaccharides are commonly found in CF lung mucus and may also bind small molecules.[3]

Despite the clinical importance of small molecule binding to mucus, relatively little is known about the chemical properties that regulate small molecule binding. What is known has largely been inferred from diffusion measurements: slower diffusion in mucus indicates increased mucus binding, since small molecules are smaller than the mesh size of mucus.[2] In these experiments, increased hydrophobicity typically correlates with slower drug diffusion.[11] Lipids, and the hydrophobic domains of mucins, are believed to account for this slowed diffusion by binding to hydrophobic drugs[2,3,5,12] although the glycans grafted to mucins may also play a role.[9] Drug charge only appears to play a major role for highly cationic molecules such as aminoglycoside and polymyxin antibiotics (+5 molecular charge in the case of the anti-*P. aeruginosa* antibiotics tobramycin and colistin).[13−18] This binding is believed to be mediated by the polyanionic glycosylated

Received: October 3, 2018
Revised: January 17, 2019
Published: February 19, 2019

DOI: 10.1021/acs.biomac.8b01467
Biomacromolecules 2019, 20, 1505−1513

domains of mucins and, in CF, eDNA, and bacterial polysaccharides.[3,5]

However, beyond an apparent correlation between diffusion and hydrophobicity, and electrostatic binding of highly charged molecules, few details are known about which molecules can bind mucus. One primary reason for this knowledge gap is that studies of mucus-small molecule interactions typically use small data sets, with fewer than 20 molecules per study (with one interesting exception that measured 41 molecules[19]).[20,21] This low volume of data is due to the difficulty of acquiring large amounts of mucus or mucus-like models. In addition, diffusion and binding measurements have been based on molecular detection techniques such as radiolabeling, fluorescence, or electrochemical methods,[20] which cannot be easily multiplexed. Thus, a data-driven approach to identifying molecules that bind mucus has so far not been feasible.

Our goal in this work is to overcome this limitation by analyzing the binding of small molecules to mucus components, including MUC5AC, DNA, and alginate, in a relatively high throughput manner. To do this, we developed an equilibrium dialysis (ED) technique to measure binding of small molecules to these biopolymers. This label-free technique can measure up to 20 molecules in a single experiment, minimizing sample volume requirements and enabling the generation of a large data set (96 molecules in total), which constitutes a substantial increase over previous studies of drug−mucus interactions.

First, we validated the biological relevance of our binding assay by showing that the cationic polymyxin antibiotic colistin binds MUC5AC, a prominent lung mucin,[6] but not the neutral polysaccharide methylcellulose (MC), and that binding was associated with inhibition of antibiotic activity. Next, we used a small molecule microarray (SMM) approach[22] to screen for MUC5AC binding of thousands of molecules, which revealed a previously unknown chemical motif associated with mucin binding. We used our novel ED method to confirm the importance of this motif in mucin binding and further showed that charge and hydrophobicity play a context-dependent role in predicting binding. Together, these findings demonstrate the strength of our technique for enabling a data-driven approach to understanding mucus binding, and illustrate important insights about the effect of mucus on small molecules.

EXPERIMENTAL SECTION

Buffer Preparation and Specifications. Phosphate-buffered saline (10×, PBS) was purchased from AccuGene. At 1× concentration, it consisted of 1 mM KH_2PO_4, 2 mM Na_2HPO_4, and 150 mM NaCl at pH 7.4. Phosphate-citrate buffer (PCB) at 1× consisted of 10 mM each of phosphate and citrate, and 58 mM sodium, at pH 7.0.

Mucin Preparation and Fluorescent Labeling. MUC5AC was purified from fresh pig stomach scrapings as described in Celli et al.,[23] with the exception that the cesium chloride density gradient ultracentrifugation step was only performed for mucin used in the SMM, not for mucin tested using ED. Briefly, mucus was scraped from fresh pig stomachs (Research 87, Inc., Boylston, MA, U.S.A.) and mucins were purified using size exclusion chromatography.

To fluorescently label the mucin, 0.6 mg was solubilized in 300 μL of pH 9 0.1 M sodium bicarbonate buffer overnight at 4 °C. Alexa Fluor 647 succinimidyl ester (ThermoFisher Scientific) dissolved in dimethyl sulfoxide (DMSO) at 10 mg/mL was added to the mucin solution to a concentration of 0.02 mg/mL (1:100 mass ratio with respect to the 2 mg/mL mucin), and the mixture was incubated at room temperature for 1 h with shaking. An equal volume of 50 mM tris(hydroxymethyl)aminomethane was added to quench the reaction and the mixture was left at room temperature for 5 min with shaking. The volume was diluted to 20 mL with PBST (PBS with Tween 20) in a Corning Spin-X 100 kDa molecular weight cutoff ultrafiltration concentrator (Fisher) and centrifuged at 3000*g* for 25 min at 4 °C; the flow-through was discarded. These steps (dilute to 20 mL with PBST, centrifuge, discard flow-through) were repeated twice more; the volume remaining after each centrifugation was approximately 5 mL. The labeled mucin was then diluted to the appropriate concentration.

Equilibrium Dialysis. ED was performed with a 12 kDa cutoff Rapid Equilibrium Dialysis device (Thermo Scientific) with 100 μL of 5 mg/mL biopolymer solution or gel, or buffer control, in the sample chamber and 300 μL of matching buffer in the assay chamber. Each experiment began with equal concentrations of the relevant compound cocktail loaded in both chambers ("1× concentration"). A 1× concentration was 200 nM for every molecule except colistin (10 μM). Equilibration took place over 4 h with shaking at 235 rpm and 37 °C, at which point aliquots were collected from the assay chamber. HPLC separation took place on an Acclaim PolarAdvantage column (3 μm pores, 2.1 × 100 mm, VWR). The HPLC method is given in Table S1. The first 5 min of eluent were diverted to a waste container to avoid salt contamination of the mass spectrometer (Agilent 6410 triple quadrupole), and the rest of the eluent was analyzed using multiple reaction monitoring (MRM). Source parameters were as follows: temperature 350 °C, gas flow 10 L/min, nebulizer 25 psi, capillary voltage 4000 V, with molecular ions and fragments for all experiments given in Tables S2−S4. Multiple transitions were tracked for several of the molecules (including colistin) as a consistency check; only one was used for analysis but all gave consistent results (not shown). Peak areas for each molecule's chromatogram were compared to an external standard curve to measure concentrations of each molecule.

The SMM and NIH Clinical Collection (NCC) compound sets (acquired from ChemBridge [San Diego, CA] and NIH respectively) were tested for biopolymer binding in 3 and 2 groups, respectively, with one exception. The assigned groupings are given in Tables S2−S3 ("Cocktail Group 1" and "Cocktail Group 2" respectively). There were 18 compounds in each group (cocktail) for the SMM runs and 20 or 21 compounds in the NCC drug cocktails, except for the experiments with SMM molecules binding to mucin in PCB, where 96 compounds (see main text) were run in 4 groups of 24 molecules each ("Cocktail Group 2" in Table S2) of which 54 molecules were successfully measured. These 54 in the 3 groups of 18 were used for all remaining experiments. The NCC consists of over 700 compounds; 41 molecules were selected randomly with the constraint that molecules with the same mass could not be included in a single cocktail, to ease qLCMS analysis. Several DAP-containing molecules were included in the NCC set (they did not bind mucin significantly more than non-DAP containing NCC molecules; not shown).

The uptake ratio R_U of a compound was calculated by (see text in the Supporting Information for derivation):

$$R_U = 1 + 4\left(\frac{1}{c_E} - \frac{1}{c_C}\right) \tag{3}$$

where c_E is the concentration in the assay chamber of the experimental dialysis system and c_C is the concentration in assay chamber of the buffer−buffer dialysis control. c_E and c_C were both scaled with respect to the 1× concentration. c_E and c_C were each averaged over three wells for one full biological replicate of R_U, which was then converted to ΔG, so $n = 3$ represents nine measured wells.

We used a biopolymer concentration of 0.5% w/v (5 mg/mL). A total of 5 mg/mL is consistent with typical mucin concentrations in lung mucus (0.1−20 mg/mL, depending on disease state[6,24−26]) and DNA concentrations in CF sputum (0.5−5 mg/mL[24,25]). It is higher than the bulk concentration of alginate in *P. aeruginosa*-infected CF sputum (0.004−0.1 mg/mL[27]), but the local concentration in a *P. aeruginosa* biofilm may approach 5 mg/mL. Alginate (MW 120−190 kDa) and calf thymus genomic DNA were purchased from Sigma.

DOI: 10.1021/acs.biomac.8b01467
Biomacromolecules 2019, 20, 1505−1513

Small Molecule Microarray. SMM slides were prepared as previously described in Bradner et al.[28] The experimental protocol was also as described in Bradner et al. using procedure steps 21A ("Dish method"), 22A ("Direct detection of fluor-labeled proteins"), and 23, with the following modifications: PBST and PBS (for the final rinse) were used instead of TBST and TBS, slides were incubated at room temperature rather than 4 °C, 5 mL of protein and wash solution was used rather than 3 mL, and 3 washes were performed instead of 2 in step 22A(i). The slides were scanned for Alexa 647-labeled mucin fluorescence using a GenePix scanner (Molecular Devices) and analyzed by GenePix Pro software (Axon Instruments). Each printed feature's signal−background ratio was quantified (on a per-feature basis per Bradner et al.) and normalized to a z-score with mean and standard deviation measured for all molecules under that feature's condition (mucin and detergent concentration).

For the initial SMM screen, each molecule appeared 16 times: twice on each slide where present and under eight conditions. Six conditions were experimental, 0.1, 0.5, and 1 μg/mL mucin with 0.05% and 0.2% Tween 20, and two conditions were controls, a PBST-only blank (0.2% Tween 20) and a fluorophore-only control (0.05% Tween 20). Spots with a z-score of 2 or more were determined to indicate binding. A molecule was considered a hit if it appeared as positive on 6 or more of the 12 potential experimental locations, but none of the four potential control locations. This combination of z-score cutoff and hit calling was selected to yield a manageable number of hits for ED analysis. For the follow-up screen, there was only one condition (0.5 μg/mL mucin, 0.1% Tween 20), but each molecule was present on two slides. A molecule was considered a hit if it had a z-score of 2 or more in all 4 possible locations. For quality control, this screen also included 144 blanks that were DMSO-only negative controls, each spotted at either 8 or 16 locations. None of these negative controls had a z-score greater than 2 in 3 or more locations, meaning that none of the negative controls were false positives (data not shown).

Computational Molecular Analysis. Motif analysis was performed using RDKit (RDKit: Open-source cheminformatics; http://www.rdkit.org) for Python. Molecules were checked for presence of DAP using the substructure query "NC1=NC=CC(N)=N1". Fisher's exact test was performed using the SciPy package.

Molecular charge was calculated as the average charge weighted by abundance over all generated protonation microspecies using the MajorMicrospeciesPlugin Calculator Plugin, Marvin 5.4.1, 2011, ChemAxon (http://www.chemaxon.com).

ClogP was calculated using BioByte (BioByte Corp, Claremont, CA).

Generation of Plots for Local and Global Correlations with Molecular Properties. We generated random "ΔG" values using 40 uniformly distributed random numbers evenly spaced between 0 and 10 (0−10 was the arbitrarily scaled x axis), and made the function continuous with a cubic spline interpolation. We generated random "Property" values using 15 normally distributed random numbers evenly spaced between 0 and 10, also with a cubic spline interpolation. The blue and red "molecules," or locations on the x axis, were selected by hand to illustrate that local and global correlations between ΔG and a molecular property may not be consistent. All figure preparation was done using Matlab (2015a, The MathWorks, Inc., Natick, MA, U.S.A.).

Colistin Activity in Mucin. Colistin MIC was first determined using a modified broth microdilution assay. *P. aeruginosa* strain PAO1 was grown overnight in BBL Mueller-Hinton II broth (MHB; BD Falcon) at 37 °C. Colistin (Sigma) stock solution was prepared at 10 mg/mL in water, then serially diluted 2-fold into MHB. The overnight culture was diluted to a final concentration of approximately 3×10^4 CFU/mL into fresh MHB. A total of 90 μL of this inoculum was added to each well of a 96-well plate with 10 μL of the colistin dilution series, such that the final concentrations evaluated were between 1 mg/mL and 0.4 μg/mL. After incubation at 37 °C for 24 h, the MIC of colistin in MHB was determined as 8 μg/mL, by visually inspecting the plate to identify the lowest concentration at which there was no visible cellular growth.

To compare the efficacy of colistin in mucin, methylcellulose, and MHB alone, PAO1 was grown overnight in MHB at 37 °C. The overnight culture was diluted to a final concentration of approximately 6×10^4 CFU/mL into fresh MHB. A total of 45 μL of this inoculum was added to each well of a 96-well plate. A total of 45 μL of either mucin (1% w/v, dissolved in MHB), methylcellulose (1% w/v, dissolved in MHB), or MHB were added to each well depending on the condition, and then 10 μL of colistin diluted into MHB was added to a final concentration was 8 μg/mL (MIC) or 16 μg/mL (2 × MIC). After incubation at 37 °C for 24 h, the number of surviving cells in each condition was evaluated by scraping the wells, homogenizing the contents by pipetting up and down vigorously, serial dilution, plating, and counting colony forming units (CFUs).

Statistical Analysis and Plots. Except for the Fisher's exact test, statistical analysis and plotting was performed in R. [R Core Team (2017). R is a language and environment for statistical computing. R Foundation for Statistical Computing, Vienna, Austria. URL https://www.R-project.org/.] Tests of significant correlation were performed using F tests. Pairwise comparison of regression coefficients was performed by testing the ability of a property to predict the difference in ΔG between two different gels. For example, a test of the model:

$$\mathrm{lm}((\mathrm{Mucin\_dG} - \mathrm{DNA\_dG}) \sim \mathrm{Charge}, \mathrm{data} = \mathrm{all\_data})$$

would test the significance of a pairwise comparison between the effect of charge on mucin and DNA binding. All tests were two-tailed.

For the ED experiments, the binding of each molecule was measured three times, as described in "Equilibrium Dialysis" of the Experimental Section.

Data Availability. The data sets generated during the current study are available from the corresponding author on request.

Code Availability. The code written and used for data analysis for the current study is available from the corresponding author on request.

RESULTS AND DISCUSSION

Development and Validation of Equilibrium Dialysis Technique to Measure Biopolymer Binding. In the ED assay, we measured the partitioning of molecules across a dialysis membrane between an assay chamber containing buffer and a sample chamber containing the biopolymer of interest in the same buffer. We used multiple compounds in the same experiment (Figure 1a) under dilute conditions to minimize competition for binding sites. We then used quantitative liquid chromatography−mass spectrometry (qLCMS) to measure molecule concentrations and quantify the equilibrium partitioning. qLCMS quantitation allowed us to measure up to 20 molecules in a single experiment.

We could not measure molecular concentrations in the sample chamber because the biopolymers were not compatible with LC. Instead, we observed binding by comparing the concentration of molecules in the assay chamber to the concentration of molecules in the assay chamber of a buffer−buffer control well (Figure 1a, Experimental Section). From these measurements, we calculated the equilibrium uptake ratio R_U, given by

$$R_U = [\mathrm{compound}]_{\mathrm{sample}}/[\mathrm{compound}]_{\mathrm{assay}} \quad (1)$$

Log-transforming R_U gives a value akin to an energy:

$$\Delta G_{\mathrm{uptake}}/k_B T = -\ln R_U \quad (2)$$

For simplicity, we consider the unitless quantity ΔG scaled by thermal energy $k_B T$, meaning $\Delta G = \Delta G_{\mathrm{uptake}}/k_B T$. This quantity is more likely than R_U to scale linearly with molecular properties that affect binding energies, so it is a better

DOI: 10.1021/acs.biomac.8b01467
Biomacromolecules 2019, 20, 1505−1513

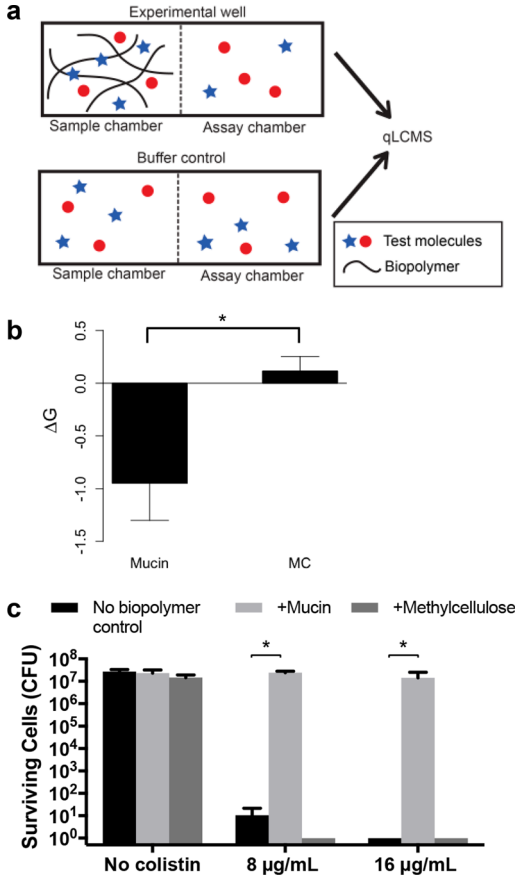

Figure 1. (a) Schematic of equilibrium dialysis (ED). Concentration in assay chamber of ED device is compared to that from a buffer control using qLCMS. Multiple compounds may be tested at once. Here, two are shown: a compound that binds mucin (blue stars) and a compound that does not (red circles). (b) Binding of colistin to mucin and methylcellulose (MC); negative ΔG implies binding. Colistin binds mucin but not MC. Error bars: SEM *p = 0.48 (t = 0.85, df = 2). (c) Surviving *P. aeruginosa* strain PAO1 cells (CFU = colony forming units) after 24 h of growth with colistin in biopolymer-free Mueller-Hinton broth (MHB), in mucin (0.5% w/v dissolved in MHB), or MC (0.5% w/v dissolved in MHB). Colistin activity is inhibited by mucin, but not by MC. No colistin control shows that mucin does not increase growth in the absence of antibiotic. *p < 0.0001.

representation of binding data for the regression analyses that follow. A negative ΔG implies binding, with more negative ΔG meaning tighter binding and an increased binding site density.

We first tested the utility of this assay using colistin, a cationic polymyxin antibiotic that has been tested clinically as an inhaled treatment for *P. aeruginosa* infection in CF.[29] Our binding measurements revealed that colistin bound to mucin but not to MC (a neutral biopolymer) at 0.5% w/v (Figure 1b; we retained this biopolymer concentration throughout this entire work, see Experimental Section). This is consistent with expectations, given colistin's +5 charge.

Next, we showed that these binding measurements correlated with differential activity against *P. aeruginosa*. We incubated *P. aeruginosa* with colistin in biopolymer-free Mueller Hinton Broth (MHB), mucin, and MC for 24 h. As predicted, mucin inhibited the effect of colistin to a substantial degree, while MC had a negligible effect on colistin bioactivity (Figure 1c). These data demonstrate that binding measurements can identify instances where mucus inhibits a drug by binding and sequestering it, which has important implications for mucosally administered drugs.

Beyond the use of our novel method to predict the effects of mucus on bioactivity for a tested molecule, the ability to predict and guide alterations that would affect mucus binding of untested molecules would be an important advance. While we measured binding of 96 molecules with ED in this work, a substantial increase in throughput over previous techniques, this still constitutes a sparse sampling of chemical space.

Identification of a Mucin Binding Motif by Small Molecule Microarray. Toward this end, we used a small molecule microarray to screen for mucin-binding small molecules (Figure 2a, Experimental Section). The glass slides were spotted with an array of covalently attached small molecules with drug-like properties: molecular weights typically between 250 and 400 Da, charge between ±2, and moderate hydrophobicity. We first ran an SMM assay on 4160 molecules, and then expanded to a set of 45,656 molecules with similar molecular properties to the initial screen. Both assays were performed in phosphate-buffered saline with Tween 20 added (PBST).

From the initial SMM, we identified 60 putative mucin binding molecules or "hits." Inspection of the structures revealed one motif that was strongly overrepresented in the hits over the nonhits (risk ratio 21.9, $p \sim 10^{-28}$, Fisher's exact test without multiple hypothesis testing correction). We termed the motif 2,4-diaminopyrimidine (DAP; Figure 2c,d; Table S5 for descriptive statistics). The DAP motif was also highly overrepresented within the 140 hits in the second, expanded SMM screen (risk ratio 9.3, $p \sim 10^{-23}$).

Equilibrium Dialysis Supports the Presence of Mucin Binding Motif. We validated the importance of DAP using ED, a more robust method than the SMM. To do this, we selected 96 molecules: the 60 hits from the initial screen, along with 36 assay negatives that include a large number of molecules containing DAP. Of these 96 molecules, 54 were amenable to measurement with qLCMS (Table S6; the others did not ionize sufficiently or were chromatographically nonseparable from inorganic salt). We used our ED method to measure binding of these molecules to mucin under two pH and ionic strength conditions: PBS (ionic strength ~ 160 mM, pH 7.4) and a lower salt phosphate−citrate buffer (PCB; 60 mM Na^+ was the sole cation) at pH 7. Exact buffer compositions are given in the Experimental Section. These two buffers capture some relevant physiological variation: salt levels in lung mucus are typically isotonic or slightly hypotonic with respect to plasma,[24,30] while pH of lung mucus is neutral to slightly basic for healthy people and slightly acidic in CF patients.[31] For binding to mucin in PCB, the average ΔG was lower for molecules with DAP than for molecules without (p = 0.0043, $F_{1,50}$ = 8.9), meaning that the presence of DAP was positively correlated with increased mucin binding, though this relationship did not hold in PBS (Figures S1 and S2). Thus, DAP is indeed associated with mucin binding and this effect is dependent on ionic composition. The higher ionic strength of PBS is the most likely explanation for the difference in binding, although the slight pH difference may have an effect; the relatively low concentration of potassium in our PBS (1 mM) is unlikely to have a significant impact.

Molecular Properties beyond DAP Affect Mucin, DNA, and Alginate Binding. We next addressed two questions: first, to what extent is binding to mucin distinguished from binding to other mucus-associated

DOI: 10.1021/acs.biomac.8b01467
Biomacromolecules 2019, 20, 1505−1513

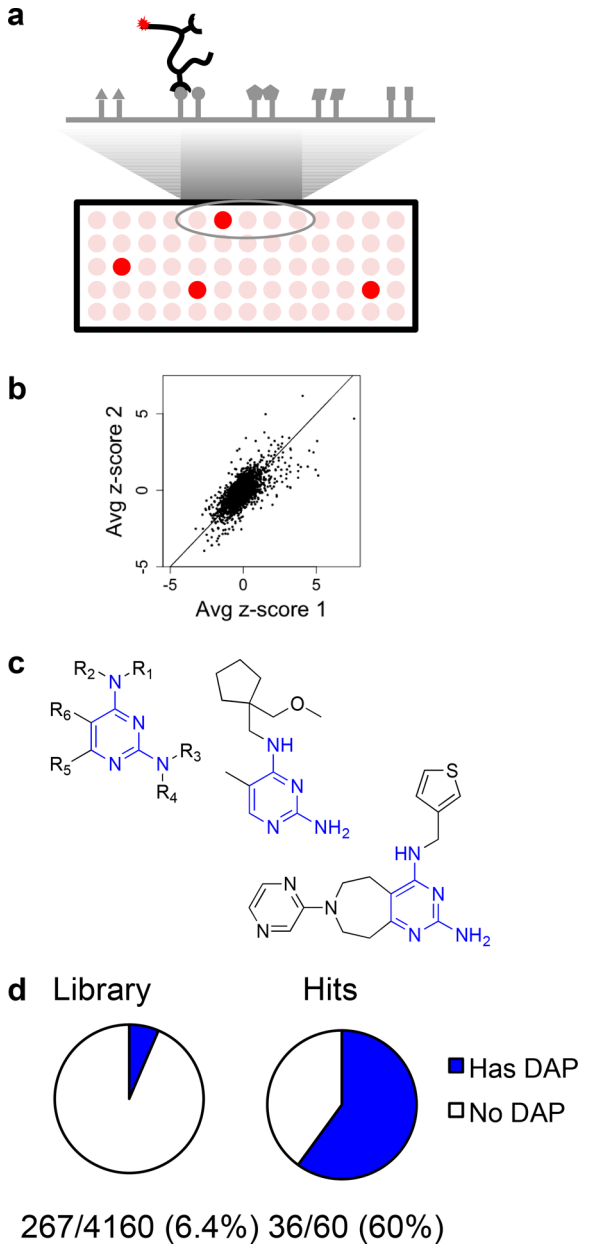

Figure 2. (a) Schematic of small molecule microarray (SMM): fluorescently labeled mucin was incubated with slides covalently linked to small molecules at defined locations. After washing and imaging, fluorescent spots on the slide indicated binding of molecule to mucin. (b) Correlation (ρ = 0.65) between average z-scores from two separate SMM experiments indicates high reproducibility. (c) 2,4-Diaminopyrimidine (DAP) motif (blue) and two representative SMM hits with DAP. (d) Pie charts show overrepresentation of DAP in hits compared to the entire library.

biopolymers, and second, are properties beyond the presence of DAP (specifically, hydrophobicity and charge) important determinants of binding to mucus. To answer the first question, we measured binding of the same set of molecules to DNA and alginate, two polymers that are major components of CF lung mucus, and bovine serum albumin (BSA) as a nonpolyanionic control. To address the second question, we determined each molecule's predicted log octanol−water partition coefficient (ClogP; the higher the ClogP, the higher the predicted hydrophobicity) and average net charge at pH 7 (for PCB) and 7.4 (for PBS).

The results of these experiments and analyses are presented in Figure 3, which depicts the slopes of best-fit lines for binding to each biopolymer vs the presence of DAP, net charge, and ClogP (Figure 3; full plots for each individual biopolymer-property pair given in Figures S1 and S2). In PCB, the presence of DAP was significantly correlated not only with binding to mucin but also with binding to DNA and alginate (Figure 3b), though not to BSA. Thus, DAP is not specific to mucin binding.

Charge and hydrophobicity also affect binding to the biopolymers. In both buffers, increased net charge is significantly correlated with binding to DNA and alginate, though the effect is stronger in PCB, consistent with the fact that increased ionic strength weakens electrostatic interactions. Moreover, there is a trend in the same direction for mucin in PCB (p = 0.080, $F_{1,50}$ = 3.2), although the effect of charge is weaker for mucin than for DNA and alginate (Figure 3d,e). These data suggest that (DNA-rich) CF lung mucus, and mucus with (alginate-rich) mucoid *P. aeruginosa* biofilms, will likely have different small molecule binding properties than the mucin-dominated mucus typically observed in COPD and asthma.[7] Increased ClogP was also correlated with stronger binding to each of the biopolymers in PCB (Figure 3f), which is consistent with previous observations that increased hydrophobicity leads to greater mucus binding.[11]

Some caution is required in interpreting these single-variable plots, as there is substantial collinearity between the presence of DAP and the other descriptors (Figure S3a−c). However, these results all hold true when restricting our data set to only molecules with DAP (Figure S4). This means that mucus binding of the tested molecules containing DAP could be modulated by the presence of charged and hydrophobic groups elsewhere on the molecular structure.

ED Experiments Across a More Chemically Diverse Set Reveal Multiple Previously Unknown Mucin Binding Molecules. Finally, we tested whether the results related to charge and hydrophobicity would apply to molecules that were more structurally diverse, since our ED experiments focused mainly on molecules with DAP. We selected 41 molecules that were amenable to qLCMS analysis from the NIH Clinical Collection (NCC), a library of clinically tested drugs and measured their binding to mucin, DNA, alginate, and BSA in PBS. Interestingly, none of the trends we observed in Figure 3 held for this more diverse set of molecules (Figure 4a,b), suggesting that there are not monotonic relationships between binding, hydrophobicity, and charge across all chemical structures. However, we did identify several molecules able to bind to mucin (Figure 4c), which may reflect mucin binding scaffolds beyond DAP that were unidentified or untested in the SMM. The lack of clear trends observed in the NCC data set suggests that correlations between charge or hydrophobicity and binding to mucus may hold locally, but not globally, in chemical space (Figure 4d−f). This makes sense if one considers that the molecules in the SMM set (which had relatively low chemical diversity) likely bind the same or similar regions on a biopolymer (such as an anionic glycosylated region of mucin) and/or with the same orientation (such as intercalated into DNA). In this case, adding or subtracting hydrophobic groups or charge would be expected to have a systematic effect on binding dictated by the common biopolymer binding site. In contrast, for molecules with vastly different scaffolds, such as the ones shown in Figure 4c, binding sites and conformations would be more varied,

DOI: 10.1021/acs.biomac.8b01467
Biomacromolecules 2019, 20, 1505−1513

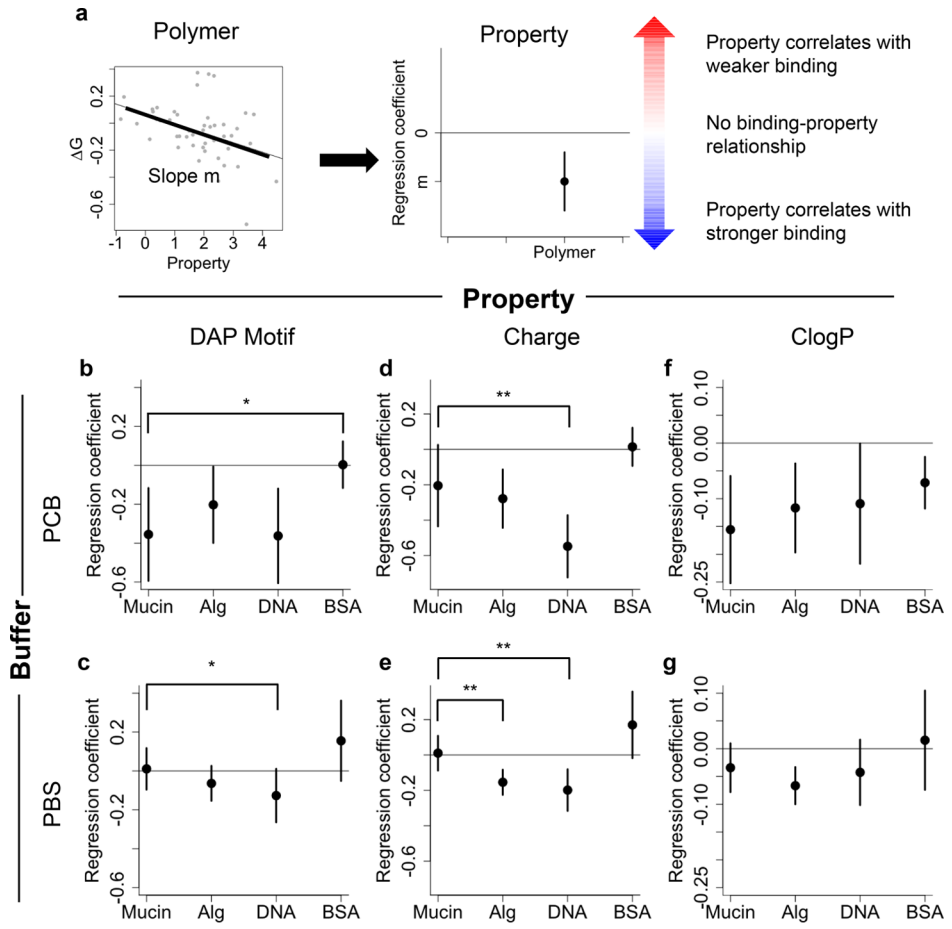

Figure 3. Effects of molecular properties on binding of small molecules to mucin, alginate ("Alg"), DNA, and BSA in PBS and PCB. (a) Schematic of analysis technique. Regression coefficient for linear model of ΔG of binding to a biopolymer against a particular molecular property (charge, ClogP, or the presence of DAP) is plotted with 95% confidence intervals. Plot on left: each individual point represents a molecule whose binding was measured along with a molecular property; charge and ClogP can be real numbers as shown in the plot, while the presence of DAP is an indicator variable, either 0 or 1. Negative and positive slopes show that increases in the predictor are associated with stronger or weaker binding, respectively. If a confidence interval does not intersect with 0, association between ΔG and the property of interest is statistically significant for the relevant polymer ($p < 0.05$). (b, c) Regression coefficient comparing molecules with and without DAP in (b) PCB and (c) PBS. For example, a value of −0.4 means ΔG is 0.4 lower for tested molecules with DAP compared to those without. Pairwise comparisons test whether the effect of DAP varies with different polymers (see Experimental Section for statistical analysis). (d, e) Regression coefficient for ΔG vs predicted molecular charge in (d) PCB and (e) PBS. Negative values imply that increased charge leads to greater binding (more negative ΔG). (f, g) Regression coefficient for ΔG vs ClogP in (f) PCB and (g) PBS. Negative values mean that increased ClogP leads to greater binding. Significance for pairwise comparisons only shown for mucin vs the other polymers. $^*p < 0.05$, $^{**}p < 0.01$ for pairwise comparisons. Exact p values given in Table S7.

reducing the expectation of correlation between binding and coarse summaries of molecular properties such as charge and ClogP.

CONCLUSIONS

Binding of small molecules to mucus is an important contributor to their activity and diffusivity within mucus. Here, we described a new technique to measure dozens of binding interactions between drugs and biopolymers commonly found in healthy and diseased mucus, and identified a mucin binding motif, DAP (Table 1a).

We also showed that for the molecules containing DAP, increased hydrophobicity and charge were associated with increased binding to various constituent components of mucus (Table 1b). Interestingly, for these molecules charge was a better predictor of binding to DNA and alginate than to mucin. This shows that these biopolymers have distinct responses to charge in spite of the fact that they are all polyanions, which is a point of potential relevance for CF.

The dependence of mucus binding on molecular detail was highlighted by the diverse molecules that bound mucus components in the NCC set, where no correlation to simple descriptors of charge and hydrophobicity was evident (Table 1b). Fortunately for the future of mucus binding research in drug design, drug development projects typically progress by testing molecules with a common scaffold, meaning that structure-binding analyses take place within a restricted chemical space (similar to the SMM set) so are likely to be enlightening. Furthermore, even in the absence of structure-binding relationships or other molecular understanding, we have established a novel and valuable method to test binding of many molecules to mucus with minimal sample requirements.

We have focused here on lung mucus and MUC5AC, in particular. A similar mucin, MUC5B, has the same domain structure as MUC5AC and is also present in lung mucus and likely abundant in the lungs of CF and COPD patients.[6] The shared domain structure of the two proteins suggests they may have similar binding tendencies, but important differences may

DOI: 10.1021/acs.biomac.8b01467
Biomacromolecules 2019, 20, 1505−1513

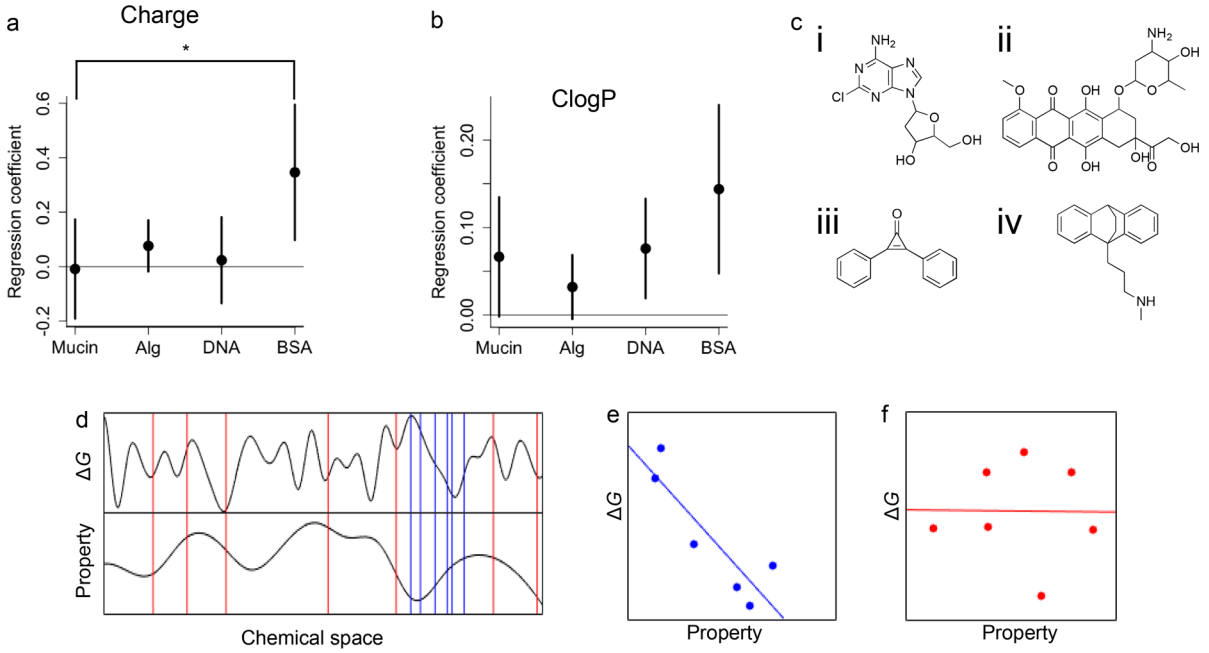

Figure 4. Effect of molecular properties on binding of molecules with diverse structures to biopolymers in PBS. (a) Regression coefficient for ΔG vs predicted molecular charge. Negative values mean increased charge leads to greater binding (more negative ΔG). (b) Regression coefficient for ΔG vs ClogP. Negative values indicate increased ClogP leads to greater binding. If a confidence interval does not intersect with 0, association between ΔG and the property of interest is statistically significant for the relevant polymer ($p < 0.05$). Significance for pairwise comparisons only tested for mucin vs the other biopolymers ($^*p < 0.05$). (c) Structures of the four strongest mucin binders ((i) cladribine, (ii) doxorubicin, (iii) diphencyprone, (iv) maprotiline) reveal no similarities: (d–f) Schematic depiction of why correlations between molecular properties (such as charge or logP) and biopolymer binding strength (ΔG) would vary depending on the molecules tested. (d) Depiction of many molecular structures projected onto one axis, which we call "chemical space," plotted against ΔG and a molecular property. Each colored vertical line represents one point in chemical space (i.e., one molecule). Blue lines depict a set of molecules with low chemical diversity (such as molecules with DAP or some other common scaffold), and red lines depict a set of molecules with relatively high chemical diversity (such as the NCC set). (e) Plot of ΔG vs the molecular property based on the blue locations shown in (a), along with best fit line. Increased values of the molecular property are locally associated with stronger binding (lower ΔG), akin to the correlation of ClogP with ΔG for molecules with DAP. (f) Plot of ΔG vs the molecular property based on the red locations shown in (d), along with best fit line. The molecular property is not globally associated with binding (ΔG), akin to the lack of correlation of charge with ΔG for molecules from the NCC set. Exact p values for (a) and (b) given in Table S7.

Table 1. Summarized Results Showing Associations between Molecular Properties and Binding to Mucin, Alginate, DNA, and BSA[a]

a			
biopolymer	correlation w/DAP		
mucin	+	+	positive correlation
alginate	+	0	no correlation
DNA	+	−	negative correlation
BSA	0		

b			
	biopolymer	correlation w/charge	correlation w/hydrophobicity
has DAP	mucin	0	+
	alginate	+	+
	DNA	+	+
	BSA	0	+
NCC set	mucin	0	0
	alginate	0	0
	DNA	0	−
	BSA	−	−

[a](a) The presence of DAP is associated with binding to mucin, alginate, and DNA but not BSA. (b) Associations of charge and hydrophobicity with binding to each biopolymer for molecules with DAP from SMM set and for molecules from the more diverse NIH Clinical Collection set.

also exist. It would therefore be an interesting extension of this work to test purified MUC5B or to more thoroughly examine mucus from mucus-secreting cell lines. Furthermore, the methods we have employed are easily transferrable to other mucus layers (such as the MUC2-rich intestine),[5,32,33] mucin-based drug delivery systems,[8] and studies of catalysis by mucin,[9] and possibly to mucus-free biopolymer systems such as biofilms.[34,35] In this vein, we have recently applied the equilibrium dialysis method to examine the binding of antibiotics to MUC5AC, MUC5B, and MUC2 and its relationship to antibiotic efficacy.[36] Our results with alginate are relevant for the activities of small molecules within biofilms, and the application of our techniques to study small molecule binding to other biofilm-associated polysaccharides such as the *P. aeruginosa*-synthesized Pel and Psl[37] is an interesting future direction. Additionally, mucus binding to other molecules such as bacterial toxins and quorum sensing molecules may be important for understanding benign and infectious microbial interactions in mucus.[38,39] Overall, the results presented here, particularly our development of an ED method to measure binding in a high-throughput manner, show that measuring and predicting mucus binding are approachable problems and promising avenues for further investigation into small molecule behavior in mucus.

DOI: 10.1021/acs.biomac.8b01467
Biomacromolecules 2019, 20, 1505−1513

■ ASSOCIATED CONTENT

Supporting Information

The Supporting Information is available free of charge on the ACS Publications website at DOI: 10.1021/acs.biomac.8b01467.

Figures S1−S4, Tables S1−S7, and a derivation of eq 4; Supporting Charts containing structures tested using ED (PDF).

■ AUTHOR INFORMATION

Corresponding Author

*E-mail: ribbeck@mit.edu.

ORCID

Jacob Witten: 0000-0003-0037-5999

Katharina Ribbeck: 0000-0001-8260-338X

Notes

The authors declare no competing financial interest.

■ ACKNOWLEDGMENTS

This work was supported by the National Institutes of Health under Award NIH R01-EB017755, the National Science Foundation under Award NSF Career PHY-1454673, and the MRSEC Program of the National Science Foundation under Award DMR-14-19807. J.W. and T.S. were supported in part by the National Science Foundation Graduate Research Fellowship under Grant No. 1122374. J.W. was supported in part by the NIH Pre-Doctoral Training Grant T32GM87232, PepsiCo Agmt 4101535548, and Novartis Agmt dtd 3/1/2018. T.S. was supported by the Siebel Scholarship and the MIT Collamore-Rogers Fellowship. We thank Collin Stultz, Al Grodzinsky, Stefan Baier, and many members of the Ribbeck lab for their helpful comments and suggestions, Andrew Chen and Angela Koehler for their helpful comments as well as providing printed SMM arrays and help with the SMMs, and Koli Taghizadeh for her help with LCMS.

■ REFERENCES

(1) Bansil, R.; Turner, B. S. Mucin Structure, Aggregation, Physiological Functions and Biomedical Applications. *Curr. Opin. Colloid Interface Sci.* **2006**, *11* (2−3), 164−170.

(2) Witten, J.; Samad, T.; Ribbeck, K. Selective Permeability of Mucus Barriers. *Curr. Opin. Biotechnol.* **2018**, *52*, 124−133.

(3) Witten, J.; Ribbeck, K. The Particle in the Spider's Web: Transport through Biological Hydrogels. *Nanoscale* **2017**, *9* (24), 8080−8095.

(4) Leal, J.; Smyth, H. D. C.; Ghosh, D. Physicochemical Properties of Mucus and Their Impact on Transmucosal Drug Delivery. *Int. J. Pharm.* **2017**, *532* (1), 555−572.

(5) Murgia, X.; Loretz, B.; Hartwig, O.; Hittinger, M.; Lehr, C.-M. The Role of Mucus on Drug Transport and Its Potential to Affect Therapeutic Outcomes. *Adv. Drug Delivery Rev.* **2018**, *124*, 82.

(6) Kirkham, S.; Sheehan, J. K.; Knight, D.; Richardson, P. S.; Thornton, D. J. Heterogeneity of Airways Mucus: Variations in the Amounts and Glycoforms of the Major Oligomeric Mucins MUC5AC and MUC5B. *Biochem. J.* **2002**, *361* (3), 537−546.

(7) Fahy, J. V.; Dickey, B. F. Airway Mucus Function and Dysfunction. *N. Engl. J. Med.* **2010**, *363* (23), 2233−2247.

(8) Duffy, C. V.; David, L.; Crouzier, T. Covalently-Crosslinked Mucin Biopolymer Hydrogels for Sustained Drug Delivery. *Acta Biomater.* **2015**, *20*, 51−59.

(9) Shraga, N.; Belgorodsky, B.; Gozin, M. Organic Reactions Promoted by Mucin Glycoproteins. *J. Am. Chem. Soc.* **2009**, *131* (34), 12074−12075.

(10) Gordon, C. A.; Hodges, N. A.; Marriott, C. Antibiotic Interaction and Diffusion through Alginate and Exopolysaccharide of Cystic Fibrosis-Derived Pseudomonas Aeruginosa. *J. Antimicrob. Chemother.* **1988**, *22* (5), 667−674.

(11) Sigurdsson, H. H.; Kirch, J.; Lehr, C.-M. Mucus as a Barrier to Lipophilic Drugs. *Int. J. Pharm.* **2013**, *453* (1), 56−64.

(12) Larhed, A. W.; Artursson, P.; Björk, E. The Influence of Intestinal Mucus Components on the Diffusion of Drugs. *Pharm. Res.* **1998**, *15* (1), 66−71.

(13) Huang, J. X.; Blaskovich, M. A.; Pelingon, R.; Ramu, S.; Kavanagh, A.; Elliott, A. G.; Butler, M. S.; Montgomery, A. B.; Cooper, M. A. Mucin Binding Reduces Colistin Antimicrobial Activity. *Antimicrob. Agents Chemother.* **2015**, *59* (10), 5925−5931.

(14) Schneider-Futschik, E. K.; Paulin, O. K. A.; Hoyer, D.; Roberts, K. D.; Ziogas, J.; Baker, M. A.; Karas, J.; Li, J.; Velkov, T. Sputum Active Polymyxin Lipopeptides: Activity against Cystic Fibrosis Pseudomonas Aeruginosa Isolates and Their Interactions with Sputum Biomolecules. *ACS Infect. Dis.* **2018**, *4*, 646.

(15) Hunt, B. E.; Weber, A.; Berger, A.; Ramsey, B.; Smith, A. L. Macromolecular Mechanisms of Sputum Inhibition of Tobramycin Activity. *Antimicrob. Agents Chemother.* **1995**, *39* (1), 34−39.

(16) Levy, J.; Smith, A. L.; Kenny, M. A.; Ramsey, B.; Schoenknecht, F. D. Bioactivity of Gentamicin in Purulent Sputum from Patients with Cystic Fibrosis or Bronchiectasis: Comparison with Activity in Serum. *J. Infect. Dis.* **1983**, *148* (6), 1069−1076.

(17) Bahamondez-Canas, T. F.; Zhang, H.; Tewes, F.; Leal, J.; Smyth, H. D. C. PEGylation of Tobramycin Improves Mucus Penetration and Antimicrobial Activity against Pseudomonas Aeruginosa Biofilms in Vitro. *Mol. Pharmaceutics* **2018**, *15*, 1643.

(18) Saggers, B. A.; Lawson, D. Some Observations on the Penetration of Antibiotics through Mucus in Vitro. *J. Clin. Pathol.* **1966**, *19* (4), 313−317.

(19) Gargano, A. F. G.; Lämmerhofer, M.; Lönn, H.; Schoenmakers, P. J.; Leek, T. Mucin-Based Stationary Phases as Tool for the Characterization of Drug−Mucus Interaction. *J. Chromatogr. A* **2014**, *1351* (Supplement C), 70−81.

(20) Khanvilkar, K.; Donovan, M. D.; Flanagan, D. R. Drug Transfer through Mucus. *Adv. Drug Delivery Rev.* **2001**, *48* (2−3), 173−193.

(21) Pontier, C.; Pachot, J.; Botham, R.; Lenfant, B.; Arnaud, P. HT29-MTX and Caco-2/TC7Monolayers as Predictive Models for Human Intestinal Absorption: Role of the Mucus Layer. *J. Pharm. Sci.* **2001**, *90* (10), 1608−1619.

(22) Hong, J. A.; Neel, D. V.; Wassaf, D.; Caballero, F.; Koehler, A. N. Recent Discoveries and Applications Involving Small-Molecule Microarrays. *Curr. Opin. Chem. Biol.* **2014**, *18*, 21−28.

(23) Celli, J.; Gregor, B.; Turner, B.; Afdhal, N. H.; Bansil, R.; Erramilli, S. Viscoelastic Properties and Dynamics of Porcine Gastric Mucin. *Biomacromolecules* **2005**, *6* (3), 1329−1333.

(24) Sanders, N.; Rudolph, C.; Braeckmans, K.; De Smedt, S. C.; Demeester, J. Extracellular Barriers in Respiratory Gene Therapy. *Adv. Drug Delivery Rev.* **2009**, *61* (2), 115−127.

(25) Suk, J. S.; Boylan, N. J.; Trehan, K.; Tang, B. C.; Schneider, C. S.; Lin, J.-M. G.; Boyle, M. P.; Zeitlin, P. L.; Lai, S. K.; Cooper, M. J.; et al. N-Acetylcysteine Enhances Cystic Fibrosis Sputum Penetration and Airway Gene Transfer by Highly Compacted DNA Nanoparticles. *Mol. Ther.* **2011**, *19* (11), 1981−1989.

(26) Henderson, A. G.; Ehre, C.; Button, B.; Abdullah, L. H.; Cai, L.-H.; Leigh, M. W.; DeMaria, G. C.; Matsui, H.; Donaldson, S. H.; Davis, C. W.; et al. Cystic Fibrosis Airway Secretions Exhibit Mucin Hyperconcentration and Increased Osmotic Pressure. *J. Clin. Invest.* **2014**, *124* (7), 3047−3060.

(27) Pedersen, S. S.; Kharazmi, A.; Espersen, F. Pseudomonas Aeruginosa Alginate in Cystic Fibrosis Sputum and the Inflammatory Response. *Infect. Immun.* **1990**, *58*, 6.

(28) Bradner, J. E.; McPherson, O. M.; Koehler, A. N. A Method for the Covalent Capture and Screening of Diverse Small Molecules in a Microarray Format. *Nat. Protoc.* **2006**, *1* (5), 2344−2352.

(29) Vardakas, K. Z.; Voulgaris, G. L.; Samonis, G.; Falagas, M. E. Inhaled Colistin Monotherapy for Respiratory Tract Infections in

Adults without Cystic Fibrosis: A Systematic Review and Meta-Analysis. *Int. J. Antimicrob. Agents* **2018**, *51* (1), 1−9.
(30) Knowles, M. R.; Robinson, J. M.; Wood, R. E.; Pue, C. A.; Mentz, W. M.; Wager, G. C.; Gatzy, J. T.; Boucher, R. C. Ion Composition of Airway Surface Liquid of Patients with Cystic Fibrosis as Compared with Normal and Disease-Control Subjects. *J. Clin. Invest.* **1997**, *100* (10), 2588−2595.
(31) Pezzulo, A. A.; Tang, X. X.; Hoegger, M. J.; Abou Alaiwa, M. H.; Ramachandran, S.; Moninger, T. O.; Karp, P. H.; Wohlford-Lenane, C. L.; Haagsman, H. P.; van Eijk, M.; et al. Reduced Airway Surface PH Impairs Bacterial Killing in the Porcine Cystic Fibrosis Lung. *Nature* **2012**, *487* (7405), 109−113.
(32) Johansson, M. E. V.; Sjövall, H.; Hansson, G. C. The Gastrointestinal Mucus System in Health and Disease. *Nat. Rev. Gastroenterol. Hepatol.* **2013**, *10* (6), 352−361.
(33) Saltzman, J.; Bendtsen, C. Modeling the Effect of Mucin Binding in the Gut on Drug Delivery. *Bull. Math. Biol.* **2018**, 1−17.
(34) Stewart, P. S. A Review of Experimental Measurements of Effective Diffusive Permeabilities and Effective Diffusion Coefficients in Biofilms. *Biotechnol. Bioeng.* **1998**, *59* (3), 261−272.
(35) Stewart, P. S. Diffusion in Biofilms. *J. Bacteriol.* **2003**, *185* (5), 1485−1491.
(36) Samad, T. S.; Co, J. Y.; Witten, J. Mucus and Mucin Environments Reduce the Efficacy of Polymyxin and Fluoroquinolone Antibiotics against *Pseudomonas aeruginosa*. *ACS Biomater. Sci. Eng.* **2019**, DOI: 10.1021/acsbiomaterials.8b01054.
(37) Billings, N.; Millan, M.; Caldara, M.; Rusconi, R.; Tarasova, Y.; Stocker, R.; Ribbeck, K. The Extracellular Matrix Component Psl Provides Fast-Acting Antibiotic Defense in Pseudomonas Aeruginosa Biofilms. *PLoS Pathog.* **2013**, *9* (8), e1003526.
(38) Smith, A. C.; Rice, A.; Sutton, B.; Gabrilska, R.; Wessel, A. K.; Whiteley, M.; Rumbaugh, K. P. Albumin Inhibits Pseudomonas Aeruginosa Quorum Sensing and Alters Polymicrobial Interactions. *Infect. Immun.* **2017**, *85* (9), e00116−17.
(39) Darch, S. E.; Simoska, O.; Fitzpatrick, M.; Barraza, J. P.; Stevenson, K. J.; Bonnecaze, R. T.; Shear, J. B.; Whiteley, M. Spatial Determinants of Quorum Signaling in a Pseudomonas Aeruginosa Infection Model. *Proc. Natl. Acad. Sci. U. S. A.* **2018**, *115* (18), 4779−4784.

DOI: 10.1021/acs.biomac.8b01467
Biomacromolecules 2019, 20, 1505−1513